Contribution from the School of Chemical Sciences, University of Illinois, Urbana, Illinois 61801

Copper(II) and Vanadyl Complexes of Binucleating Ligands. Magnetic Exchange Interactions Propagated through an Extensive Organic System

ELVIRA F. HASTY, THERESE J. COLBURN, and DAVID N. HENDRICKSON*

Received February 2, 1973

Two new planar binucleating ligands were prepared from the reaction of either 1,2,4,5-tetraaminobenzene or 3,3′,4,4′-tetraaminobiphenyl and the condensation product of triethyl orthoformate and acetylacetone. The variable-temperature (4.2–216°K) magnetic susceptibility curve of the tetraaminobenzene-bridged Cu(II) dimer exhibited an antiferromagnetic interaction ($J = -12.2$ cm^{-1}), whereas no interaction was detected in the curve for the tetraaminobiphenyl-bridged Cu(II) dimer. The intramolecular nature of the superexchange was demonstrated by recourse to susceptibility curves which showed no interaction for four monomeric copper complexes with very similar environments and by esr studies at liquid nitrogen temperature of the tetraaminobenzene-bridged Cu(II) dimer doped into a dimeric Ni(II) host. An $A_{\parallel}$(Cu) value equal to one-half that in a monomer Cu(II) complex was clear indication of intramolecular exchange. Zero-field splitting was also visible in the parallel part of the esr spectrum of the Cu(II) dimer. The magnetic susceptibility curve of the tetraaminobenzene-bridged binucleated vanadyl dimer did not show any indications of exchange interactions. The esr of this vanadyl dimer in a frozen glass only exhibited zero-field splitting. An explanation of the apparent difference in exchange interaction between the copper and vanadyl dimers is advanced.

Introduction

Harris, Sinn, and coworkers, in a series of ten papers,[1] have been investigating metal complexes as ligands. Employing various Schiff base-metal complexes as ligands, they have been able to prepare many square-planar binuclear and trinuclear complexes containing similar and dissimilar metals. Other workers[2-4] have reported the preparation and properties of similar binuclear complexes. The main thrust of all of these studies has been the characterization of the complexes by variable-temperature magnetic susceptibility. Antiferromagnetic interactions propagated through ~90°

bridges have been detected for most of the complexes. Recently various workers have prepared ligands which will simultaneously bind two metal ions. These binucleating ligands afford, in many cases, metal complexes possessing environments that are very similar to those encountered in the above work; however, in general, different bridging groups and geometries can be incorporated in the latter compounds. Two justifications have been advanced for studying the metal complexes of binucleating ligands. On the one hand Robson and coworkers[5-8] are concerned with the potential reactivity of such binucleated metal complexes toward small ions and neutral molecules. Other workers[9-12] are concerned with the electronic structure, in particular, the superexchange interaction in these complexes.

Very recently Hatfield and coworkers[13,14] reported a long-range exchange interaction between two copper(II) centers bridged by pyrazine ligands. In total six polymeric-substituted pyrazine-copper complexes were studied and the magnetic susceptibility data were fit in some cases to the Ising model for linear chains and in other cases to a model for dimers. The crystal structure of only one of these copper-pyrazine polymers has been reported.

In this paper we report the preparation and characterization of a new binucleating ligand system incorporating an extensive organic moiety as a bridge between two similar metals. Variable-temperature (4.2–290°K) magnetic susceptibility and esr have been used to study the extent of exchange interaction between either two copper(II) or two vanadyl (VO^{2+}) ions bound in the ligand.

Results and Discussion

Complexes of the Binucleating Ligands $A^4(B^3)_2H_4$ and $A^3(B^3)_2H_4$. Jager[15-19] has reported the synthesis of a series of copper(II) and nickel(II) complexes by the general reaction scheme shown as Scheme I where B and A are variables.

We have modified this scheme by replacing the diamine with the tetraamines 1,2,4,5-tetraaminobenzene (designated A^4) and 3,3′,4,4′-tetraaminobiphenyl (designated A^3). With the ligands prepared in this way we were able to make Cu^{2+} and Ni^{2+} complexes of structures I and II. Vanadyl (VO^{2+}) was only incorporated into structure I. Taking Jager's lead, we will designate complexes of structure I as $M_2A^4(B^3)_2$ and those of structure II as $M_2A^3(B^3)_2$. Analytical results for these copper, nickel, and vanadyl compounds, as well as other Jager compounds used in the following physical studies, can be found in Table I. It can be seen that the analytical data for $A^4(B^3)_2H_4$ and the complexes of the binucleating ligands are indicative of the presence of water in the com-

(1) S. Kokot, C. M. Harris, and E. Sinn, *Aust. J. Chem.*, 25, 45 (1972); earlier papers are referenced.
(2) H. Ojima and K. Yamada, *Proc. Symp. Coord. Chem., 3rd*, 1, 281 (1970).
(3) W. E. Hatfield and J. A. Crissman, *Inorg. Nucl. Chem. Lett.*, 4, 731 (1968).
(4) M. Kato, Y. Muto, H. B. Jonassen, K. Imai, and T. Tokii, *Bull. Chem. Soc. Jap.*, 43, 1066 (1970).
(5) R. Robson, *Inorg. Nucl. Chem. Lett.*, 6, 125 (1970).
(6) R. Robson, *Aust. J. Chem.*, 23, 2217 (1970).
(7) N. H. Pilkington and R. Robson, *Aust. J. Chem.*, 23, 2225 (1970).
(8) B. F. Hoskins, R. Robson, and H. Schaap, *Inorg. Nucl. Chem. Lett.*, 8, 21 (1972).
(9) J. E. Andrew, P. W. Ball, and A. B. Blake, *Chem. Commun.*, 143 (1969).
(10) H. Okawa and S. Kida, *Bull. Chem. Soc. Jap.*, 44, 1172 (1971).
(11) H. Okawa and S. Kida, *Inorg. Nucl. Chem. Lett.*, 7, 751 (1971).
(12) L. K. Thompson, V. T. Chacko, J. A. Elvidge, A. B. P. Lever, and R. V. Parish, *Can. J. Chem.*, 47, 4141 (1969).
(13) J. F. Villa and W. E. Hatfield, *J. Amer. Chem. Soc.*, 93, 4081 (1971).
(14) G. W. Inman, Jr., and W. E. Hatfield, *Inorg. Chem.*, 11, 3085 (1972).
(15) Von L. Wolf and E. G. Jager, *Z. Anorg. Allg. Chem.*, 346, 76 (1966).
(16) E. G. Jager, *Z. Anorg. Allg. Chem.*, 364, 177 (1969).
(17) E. G. Jager, *Z. Chem.*, 4, 437 (1964).
(18) E. G. Jager, *Z. Chem.*, 8, 30 (1968).
(19) E. G. Jager, *Z. Chem.*, 8, 392 (1968).

Scheme I

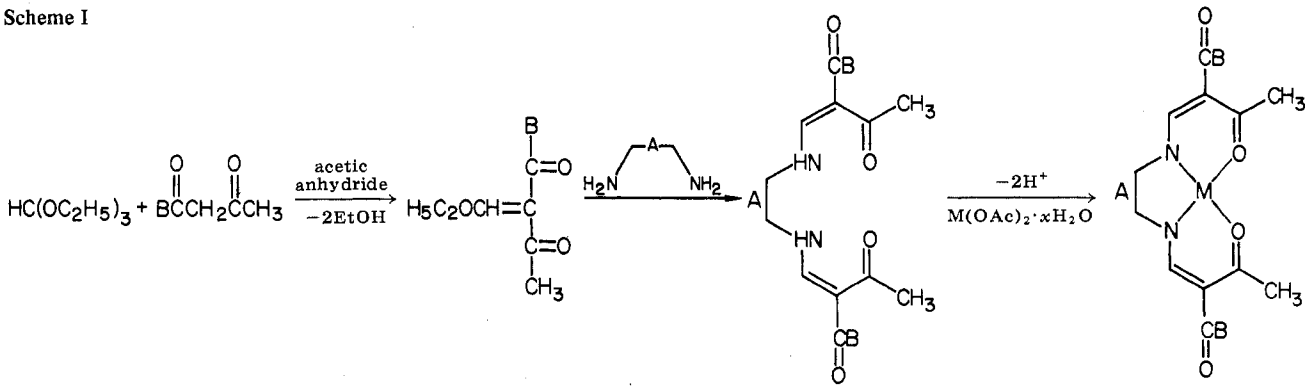

Table I. Analytical Data

Compound	% C		% H		% N		% M	
	Calcd	Found	Calcd	Found	Calcd	Found	Calcd	Found
$A^1B^3H_2$	65.85	65.95	6.09	6.11	8.53	8.55		
CuA^1B^3	55.44	55.44	4.66	5.13	7.19	7.13	16.30	15.86
CuA^1B^1	53.33	53.36	4.90	4.98	6.22	6.38	14.11	14.20
CuA^2B^3	49.19	49.03	5.27	5.22	8.20	8.21	18.57	18.41
CuA^2B^1	47.76	48.00	5.47	5.62	6.97	7.04	15.78	15.72
NiA^1B^3	56.14	55.80	4.72	4.66	7.28	7.56	15.25	15.19
VOA^1B^3	54.96	54.40	4.62	4.70	7.12	7.24	12.95	13.00
$A^4(B^3)_2H_4 \cdot H_2O$	60.38	60.61	6.09	6.18	9.39	8.98		
$Cu_2A^4(B^3)_2 \cdot H_2O$	50.06	49.63	4.49	4.44	7.79	7.59	17.66	17.67
$Ni_2A^4(B^3)_2 \cdot H_2O$	49.48	49.92	4.72	4.83	7.70	7.93	16.13	16.62
$(VO)_2A^4(B^3)_2 \cdot 2H_2O$	48.39	47.76	4.61	4.69	7.53	8.24	13.68	13.28
$A^3(B^3)_2H_4$	66.03	65.38	5.86	5.88	8.56	8.89		
$Cu_2A^3(B^3)_2 \cdot H_2O$	54.33	54.37	4.56	4.27	7.04	7.36	15.97	15.72

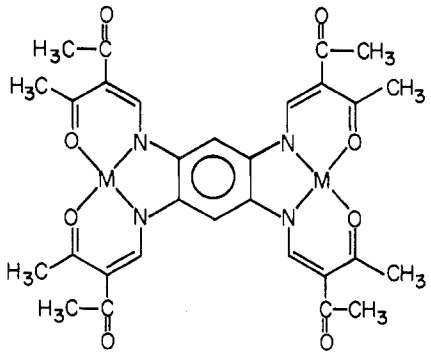

I

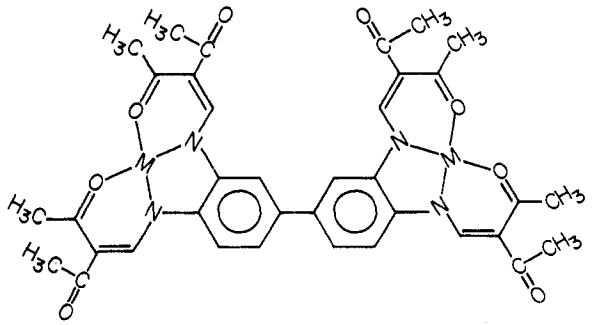

II

pounds. The presence of water is also indicated in the infrared spectra as a broad band about the 3500-cm^{-1} region. It was not possible to remove this water by either heating the complexes at 120° or drying them *in vacuo* over P_2O_5. In addition to the analytical data, further evidence supporting our formulation of the compounds is found in mass spectrometry. Both of the ligands melted at ~250°, $A^4(B^3)_2H_4$ at 252° (760 Torr), and $A^3(B^3)_2H_4$ at 246° (760 Torr); low-intensity parent peaks were detected in the mass spectra for both binucleating ligands. Mass spectra were also run for $Cu_2A^4(B^3)_2$, $Ni_2A^4(B^3)_2$, and $(VO)_2A^4(B^3)_2$, and because these complexes are less volatile it was necessary to use somewhat elevated temperatures: sample probe at 350° and source at 220°. In the case of $Cu_2A^4(B^3)_2$ a cluster of six peaks was seen at *m/e* 700–705 values with the two most intense peaks at 700 and 702. This cluster has the appearance expected (fit by a computer program) for the parent ion $Cu_2A^4(B^3)_2^+$ (mol wt = 701.7) when ^{13}C satellites and the copper isotope ratios (69.1% ^{63}Cu and 30.9% ^{65}Cu) are taken into account. No peaks with appreciable intensity were seen up to *m/e* equals 780. The nickel isotope ratios (67.8% ^{58}Ni and 26.2% ^{60}Ni) are about identical with those for copper and it was pleasing to see the highest *m/e* peak cluster for $Ni_2A^4(B^3)_2$ (690–695) to have an appearance very similar to the corresponding cluster for the copper dimer. The molecular weight of $Ni_2A^4(B^3)_2$ is 692.0. Note that in each case the water indicated by the analytical data is lost in the mass spectrometer. The vanadyl dimer did not show a parent peak.

In the following sections we will use the Jager MA^1B^3 complexes as "monomeric" counterparts of the $M_2A^4(B^3)_2$ and $M_2A^3(B^3)_2$ complexes. The local metal environments should be very similar in that $A^1B^3H_2$ is derived from 1,2-diaminobenzene and acetylacetone.

The infrared spectra of $A^1B^3H_2$ and CuA^1B^3 are reproduced in Figures 1 and 2, respectively. In going from the ligand to the copper complex the NH features are lost. These can be

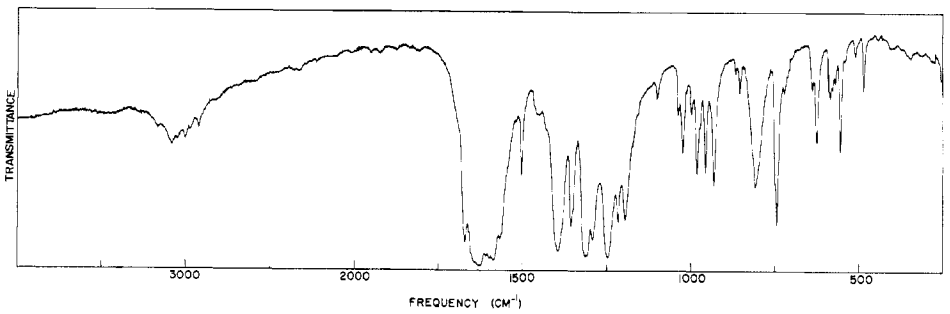

Figure 1. Infrared spectrum of $A^1B^3H_2$ (KBr pellet).

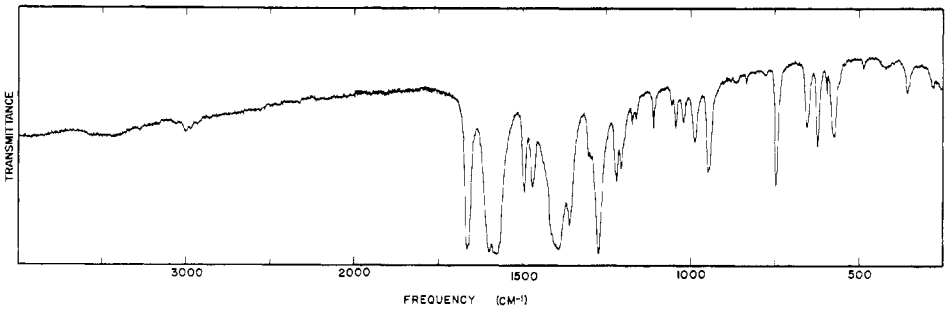

Figure 2. Infrared spectrum of CuA^1B^3 (KBr pellet).

seen in the $A^1B^3H_2$ spectrum as the band system at 3100 cm^{-1} and the band at 860 cm^{-1}. Coordination of $A^1B^3H_2$ to copper is also reflected in a splitting of a ligand ν(CO) system centered at 1625 cm^{-1} into a band for the free CO at 1664 cm^{-1} and a band system for the coordinated CO at 1580 cm^{-1}. In the CuA^1B^3 spectrum there is a Cu-N band at 358 cm^{-1} and a Cu-O band at 420 cm^{-1}. The infrared spectra of $A^4(B^3)_2H_4$ and $Cu_2A^4(B^3)_2$ are similar to those of $A^1B^3H_2$ and CuA^1B^3, respectively, and corresponding spectral changes (see Table II) are seen for the ligand $A^4(B^3)_2H_4$ upon coordination with copper.

Magnetic Susceptibilities. Magnetic susceptibilities were determined for four monomeric Jager copper complexes (CuA^1B^3, CuA^1B^1, CuA^2B^3, and CuA^2B^1) as a function of temperature in the range of 4.2–290°K. The data are given in Table III. All four of these monomeric copper complexes have μ_{eff} values that are typical for Cu(II) and are relatively temperature independent. There is no evidence for intermolecular exchange interactions present in these four planar copper complexes. Hatfield and coworkers[20] have reported many instances of intermolecular interactions between planar copper molecules. Apparently in these CuA^xB^y compounds the molecules do not pack such that there is an intermolecular

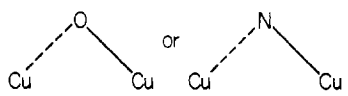

interaction.

The susceptibility *vs.* temperature curve for "binucleated" $Cu_2A^4(B^3)_2$ is depicted in Figure 3 and the data are given in Table IV. The magnetic susceptibility for this compound increases with decreasing temperature until a maximum in χ is reached at 24°K. Below this temperature the magnetic susceptibility decreases rapidly. It is clear that there is an antiferromagnetic interaction present in this compound. Because no intermolecular exchange interactions were evident in the analogous monomeric systems, it is reasonable to assign this antiferromagnetic coupling to an intramolecular interaction. In the next section we will demonstrate with esr that

(20) D. Y. Jeter, D. J. Hodgson, and W. E. Hatfield, *Inorg. Chem.*, 11, 185 (1972); W. E. Hatfield, *ibid.*, 11, 216 (1972); W. E. Hatfield and G. W. Inman, Jr., *ibid.*, 8, 1376 (1969).

Table II. Infrared Spectral Bands of $A^4(B^3)_2H_4$ and $Cu_2A^4(B^3)_2$

$A^4(B^3)_2H_4$	$Cu_2A^4(B^3)_2$	Assignment
~3500 br	~3500 br	ν OH (H_2O)
3060 w		ν NH
~3000 w	~3000 w	ν CH, ν CCH_3, ν CH_3(CO)
1625 vs		ν CO, ν C=C
	1660 s	ν CO (free)
	1585 vs	ν CO (chel), ν C=C
1392 s	1400 s	ν C=C, ν CH_3C, ν CH_3(CO)
1283 vs	1280 vs	ν CN
1190 w	1190 w	ν ring
930–1020 w	950–1040 w	ring, ν CN
	430 w	ν CuO, π ring
450 vw		π ring
	350 w	ν CuN

Table III. Variable-Temperature Magnetic Susceptibility Data for Various Curie-Law Compounds[a]

	μ_{eff}				Cu_2-$A^3(B^3)_2$	$(VO)_2$-$A^4(B^3)_2$
T, °K	Cu-A^1B^3	Cu-A^1B^1	Cu-A^2B^3	Cu-A^2B^1	μ_{eff}/Cu	μ_{eff}/V
290	1.67					
266		1.76				
241	1.67		1.74	1.79	1.83	1.91
216		1.82				
191	1.72		1.79	1.86	1.86	1.88
134	1.71	1.82	1.76	1.81	1.84	1.83
105		1.85	1.78	1.83	1.87	1.82
65.8	1.68	1.82	1.79	1.84	1.82	1.76
42.2	1.68	1.81	1.79	1.83	1.82	1.80
27.7		1.81	1.83	1.87	1.79	1.84
23.5						1.83
20.2						1.83
17.0						1.86
16.5	1.62	1.77	1.71	1.74	1.75	
11.3						1.70
9.5	1.60	1.77	1.69	1.71	1.71	1.73
6.0		1.74	1.65	1.66	1.66	1.70
4.6	1.58					
4.2	1.63	1.80	1.70	1.69	1.69	1.73

[a] The effective magnetic moments (μ_{eff} in BM) were derived from molar paramagnetic susceptibilities corrected for the background and for the diamagnetism of the compound (*via* Pascal's constants).

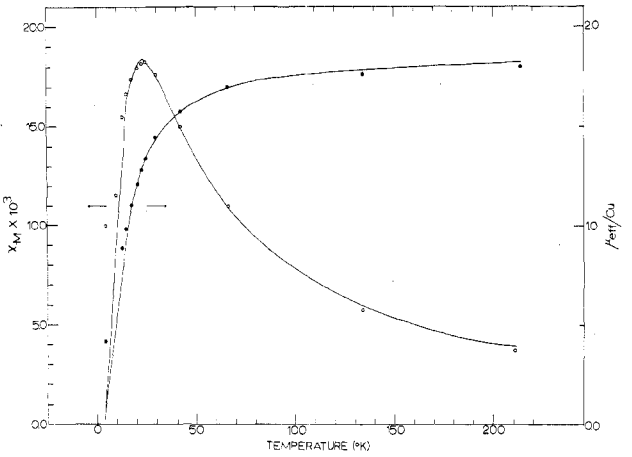

Figure 3. The temperature dependence of the magnetic susceptibility and the magnetic moment of $Cu_2A^4(B^3)_2$. The circles represent the experimental results and the solid lines represent the best fit theoretical curves calculated from STEPT (see text).

Table IV. Variable-Temperature Magnetic Susceptibility Data for $Cu_2A^4(B^3)_2$

χ_M^{cor}[a] ($\times 10^3$) (cgs units)	μ_{eff}/ Cu, BM	T, °K	χ_M^{cor}[a] ($\times 10^3$) (cgs units)	μ_{eff}/ Cu, BM	T, °K
3.741	1.80	216	18.12	1.21	20.3
5.805	1.76	134	17.50	1.11	17.5
11.04	1.70	65.7	16.76	0.99	14.5
13.95	1.53	42.2	15.62	0.89	12.7
17.79	1.45	29.5	11.62	0.66	9.5
18.37	1.34	24.5	10.41	0.42	4.2
18.33	1.28	22.5			

[a] Molar paramagnetic susceptibility corrected for background and for diamagnetism of compound. Compound diamagnetism from Pascal's constants set equal to -330×10^{-6} cgs/mol.

this is indeed the case. The molecule $Cu_2A^4(B^3)_2$ possesses a superexchange interaction propagated through the moiety

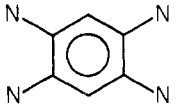

This is a larger organic framework than the pyrazine bridge

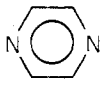

that was recently reported[13,14] to give a superexchange interaction between two Cu(II) centers. Even further, this is the first nonpolymeric Cu(II) material with an extended organic bridge that has been reported to exhibit an exchange interaction.

The magnetic susceptibility data for $Cu_2A^4(B^3)_2$ were least-squares fit to the Bleaney-Bowers equation.[21]

$$\chi_M = \frac{Ng^2\beta^2}{3k(T-\Theta)}[1 + {}^1/_3 \exp(-2J/kT)]^{-1} + N\alpha$$

In this equation χ_M is the molar paramagnetic susceptibility for a dimer and N, g, B, k, and T have their usual meaning. The intermolecular interactions are gauged by Θ, the Curie-Weiss constant. The best fit is represented in Figure 3 as a solid line, $N\alpha$ was assumed to be 120×10^{-6} cgs/mol, while the best fit parameters were found to be $J = -12.2$ cm^{-1}, $g = 2.128$, and $\Theta = -0.14°$.

(21) B. Bleaney and K. D. Bowers, *Proc. Roy. Soc., Ser. A*, **214**, 451 (1952).

In an effort to increase the size of the organic bridge, $Cu_2A^3(B^3)_2$ was prepared. In this case the bridging moiety is

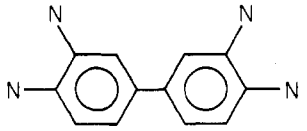

Variable-temperature magnetic susceptibility data were collected for $Cu_2A^3(B^3)_2$ and they are given in Table V. No indication of any interaction is evident in the susceptibility data for this molecule.

At present there is a shortage of variable-temperature magnetic susceptibility data for given ligand-bridge systems with different metals. We prepared $(VO)_2A^4(B^3)_2$ and measured its magnetic susceptibility as a function of temperature (see Table III). Even though the copper system exhibited an interaction, there is no sign of an interaction in the $(VO)_2A^4(B^3)_2$ data. In the last section of this paper we will discuss the exchange mechanism operative in $Cu_2A^4(B^3)_2$ and in so doing it will become clear why there is little interaction in $(VO)_2A^4(B^3)_2$.

Electron Spin Resonance. In the previous section an antiferromagnetic exchange interaction was detected in $Cu_2A^4(B^3)_2$ and it was stated that esr data indicated this interaction is intramolecular in nature. We first turn to a characterization of the "monomer." The complex CuA^1B^3 was dissolved in $CHCl_3$ and a room-temperature spectrum was obtained; it is reported in Figure 4. Four copper hyperfine lines are seen with $A_{av}(Cu) = 88.9 \pm 1 \times 10^{-4}$ cm^{-1}. The copper in CuA^1B^3 is in an N_2O_2 environment and the structure on the highest field copper hyperfine line is probably due to splitting by the two nitrogen atoms as well as one or more hydrogens. The g_{av} for CuA^1B^3 is calculated from the spectrum in Figure 4 to be 2.089.

The molecule CuA^1B^3 can be doped into diamagnetic NiA^1B^3 and in Figure 5 is reproduced the esr spectrum of a 0.1% doped sample maintained at liquid nitrogen temperature. The copper hyperfine on the parallel signal is readily visible and from it one can determine $A_\parallel(Cu) = 191.9 \pm 1 \times 10^{-4}$ cm^{-1} and with A_{av} above this gives $A_\perp(Cu) = 37.5 \pm 1 \times 10^{-4}$ cm^{-1}. The $g_\parallel$ value was calculated from the "doped" spectrum to be 2.148. The $g_\perp$ value was obtained from a pure sample to which a small amount of DPPH had been added. Extrahyperfine structure is also seen on the four parallel copper hyperfine lines; the spacing is about 6.7×10^{-4} cm^{-1}. There again seems to be more lines than is expected for two equivalent nitrogen atoms and it is necessary to consider coupling with one or more nearby protons.[22] The perpendicular region of the spectrum of doped CuA^1B^3 is quite complicated and unfortunately we do not presently have the appropriate computer simulation program to extract the desired information from this spectrum.

With a reasonably good characterization of the magnetic parameters of the "monomeric" counterpart of $Cu_2A^4(B^3)_2$ in hand, the esr spectrum of this latter compound can more properly be investigated. In Figure 6 is given a composite of the esr spectra at liquid nitrogen temperature of three "forms" of $Cu_2A^4(B^3)_2$. In the top curve is depicted the spectrum of a powdered sample of $Cu_2A^4(B^3)_2$, while in the middle tracing we have reproduced the spectrum of a doped [in diamagnetic $Ni_2A^4(B^3)_2$] sample of $Cu_2A^4(B^3)_2$. The powdered sample of the compound was mixed with a small amount of DPPH and this is visible as a spike. Finally, the

(22) A. H. Maki and B. R. McGarvey, *J. Chem. Phys.*, **29**, 35 (1958).

Table V. Summary of Electron Spin Resonance Data

Compound	Diluent	$g_\parallel$[a]	$g_\perp$[a]	$A_\parallel$[b]	$A_\perp$[b]	$a_\parallel$[b]	$a_\perp$[b]	$D_\parallel$[b]
CuA^1B^3	$CHCl_3$	2.148	2.060	191.9 ± 1.4	37.5 ± 1	6.7	7.5	
	NiA^1B^3							
$Cu_2A^4(B^3)_2$	$Ni_2A^4(B^3)_2$	2.140 ± 0.01	2.057	98.2 ± 1		6.7	7.5	24.8 ± 1
$CuNiA^4(B^3)_2$	$Ni_2A^4(B^3)_2$	2.180 ± 0.01		193.3 ± 2		6.7	7.5	
$Cu_2A^3(B^3)_2$	$A^3(B^3)_2H_4$	2.175 ± 0.01	2.074	196.0 ± 1			7.5	
VOA^1B^3	$CHCl_3$, NiA^1B^3	1.947	1.973	154.2 ± 1	51.4 ± 1			
$(VO)_2A^4(B^3)_2$	$CHCl_3$, $A^4(B^3)_2H_4$	1.938	1.959	163 ± 2	64 ± 2			
	DMSO (frozen)			159 ± 2	66 ± 2			32.5 ± 2

[a] Uncertainty ±0.001 unless stated. [b] $\times 10^4$ cm^{-1}.

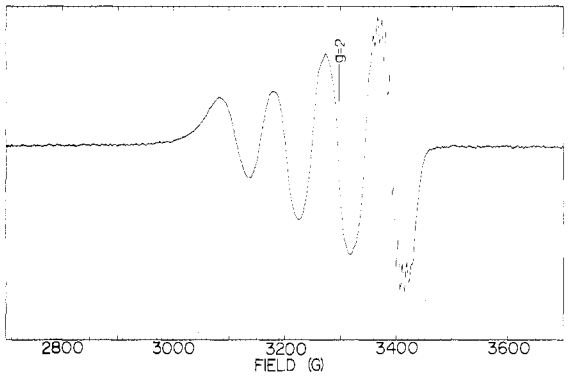

Figure 4. Esr spectrum of a CuA^1B^3 solution in $CHCl_3$ recorded at room temperature.

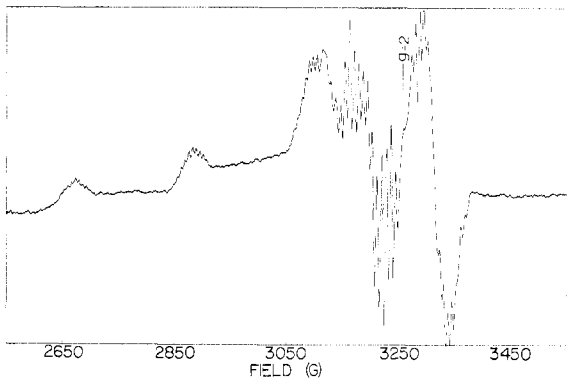

Figure 5. Esr spectrum of CuA^1B^3 magnetically diluted in NiA^1B^3 recorded at liquid-nitrogen temperature.

bottom tracing is the spectrum of $CuNiA^4(B^3)_2$ doped into $Ni_2A^4(B^3)_2$. This material was obtained by reacting a solution of the ligand with a solution containing Ni^{2+} and a small amount (1%) of Cu^{2+}. As might be anticipated the $CuNiA^4(B^3)_2$ spectrum is very similar to the spectrum of doped CuA^1B^3 in Figure 5. The N_2O_2 copper environments are very similar. The $CuNiA^4(B^3)_2$ spectrum is characterized by $A_\parallel(Cu) = 193.3 \pm 2 \times 10^{-4}$ cm^{-1}, and $g_\parallel \sim 2.18$. Structure is visible in the perpendicular region but it was not analyzed. The $Cu_2A^4(B^3)_2$ powder spectrum (top in Figure 6) gives $g_\parallel \sim 2.14$ and $g_\perp = 2.057$. The most interesting spectrum in Figure 6 is that of doped $Cu_2A^4(B^3)_2$. In the low-field part of the parallel signal it is evident, from a comparison with the spectrum of $CuNiA^4(B^3)_2$, that there are many more copper hyperfine lines than in a monomer environment. If the unpaired electrons on the two copper centers in $Cu_2A^4(B^3)_2$ are exchanging (*i.e.*, there is an intramolecular exchange interaction), 14 lines would be expected for the parallel signal. The 14 lines result from two equivalent copper ions in combination with zero-field splitting. Examination of the doped $Cu_2A^4(B^3)_2$ spectrum clearly shows there are seven lines at lower field than the $g_\parallel$ value expected for such an environ-

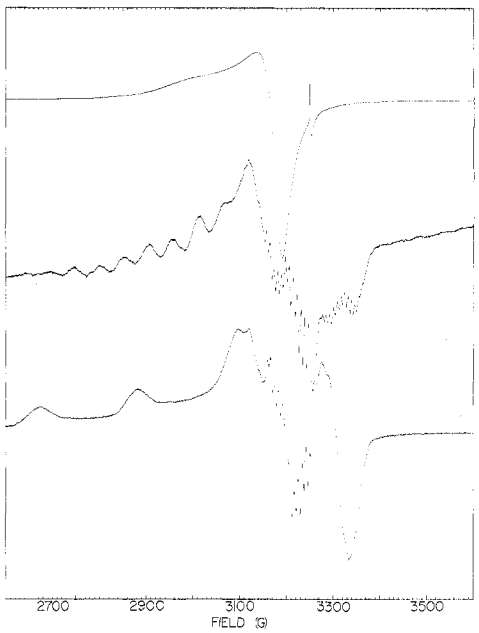

Figure 6. Composite of the esr spectra of $Cu_2A^4(B^3)_2$ recorded at liquid-nitrogen temperature: top, pure sample plus a small amount of DPPH; middle, magnetically diluted in $Ni_2A^4(B^3)_2$; bottom, magnetically diluted $CuNiA^4(B^3)_2$ in $Ni_2A^4(B^3)_2$.

ment. In Table V the magnetic parameters are given for the various copper molecules and it is clear that $g_\parallel$ is about the same for doped CuA^1B^3, doped $CuNiA^4(B^3)_2$, and powdered $Cu_2A^4(B^3)_2$. In the high-field part of the doped $Cu_2A^4(B^3)_2$ spectrum it is even possible to see the two highest field components of the 14-line parallel signal. An analysis of the parallel part of the doped $Cu_2A^4(B^3)_2$ spectrum gives $A_\parallel(Cu) = 98.2 \pm 1 \times 10^{-4}$ cm^{-1} and $D_\parallel = 2.48 \pm 0.1 \times 10^{-3}$ cm^{-1}. The magnitude of $A_\parallel$ in this complex is conclusive evidence that we are dealing with an intramolecular antiferromagnetically coupled copper dimer because it is well known[23] that the $A_\parallel$ value for a dimer will be half that of the corresponding monomer [*i.e.*, doped $CuNiA^4(B^3)_2$].

The value of the zero-field splitting parameter $D_\parallel$ can be used to determine an approximate value for the copper-copper distance in $Cu_2A^4(B^3)_2$. Zero-field splitting in such a dimer is due to a combination of dipole-dipole D_{dd} and pseudo-dipolar D_{pseudo} interactions.[21]

$$D_\parallel(\text{exp}) = D_{dd} + D_{pseudo}$$

The pseudo-dipolar interaction is generally smaller and is dependent on exchange interaction (exchange integral J) and the degree of magnetic anisotropy in the system. Its sign is opposite to that of the dipole-dipole D_{dd} interaction.

$$D_{pseudo} = 2J[((g_\parallel - 2)^2/4) - (g_\perp - 2)^2]/8$$

(23) C. P. Slichter, *Phys. Rev.*, 99, 479 (1955).

If we take the ground state exchange integral $J = -12.2$ cm^{-1} as the J value appropriate for the D_{pseudo} equation, then we calculate a value of -5.03×10^{-3} cm^{-1} for D_{pseudo}. Addition of $-D_{pseudo}$ to $D_{\parallel}$ (exp) gives $D_{dd} = 75.1 \times 10^{-4}$ cm^{-1} and this can be used to evaluate R, the Cu-Cu distance, from the following equation[24]

$$R = (0.650 g_{\parallel}^2 / D_{dd})^{1/3}$$

This gives $R = 7.36$ Å, which is reasonably close to the copper-copper distance that one finds for a model of $Cu_2A^4(B^3)_2$.

The compound $Cu_2A^3(B^3)_2$ was doped at 1% into the ligand $A^3(B^3)_2H_4$ and the liquid-nitrogen temperature esr spectrum was run (see Figure 7). This spectrum looks very similar to that for doped $CuNiA^4(B^3)_2$ (bottom in Figure 6). Variable-temperature magnetic susceptibility measurements for $Cu_2A^3(B^3)_2$ indicated that the exchange integral $|J|$ is less than 1 cm^{-1}. The esr spectrum in Figure 7 is telling us that the exchange rate is slower than the esr time scale; that is, in the dimer $Cu_2A^3(B^3)_2$ the unpaired electrons are "localized" about the two copper centers and are not exchanging. In passing we should comment on some of the esr parameters for the copper complexes as given in Table V. Kivelson and Neiman[25] have presented the theory requisite for an analysis of copper esr spectra. The values of $A_{\parallel} \sim 193 \times 10^{-4}$ cm^{-1} are greater than those found for various simple bisbidentate-copper complexes (*e.g.*, oxalate, 2,2′-dipyridyl, and 1,10-phenanthroline). In these cases the $A_{\parallel}$ values range from $\sim$150 to $\sim$170 $\times 10^{-4}$ cm^{-1}. The $A_{\parallel}$ values for the Jager complexes are, however, less than those for copper phthalocyanine (220×10^{-4} cm^{-1}) and copper tetraphenylporphin (250×10^{-4} cm^{-1}). This can be qualitatively interpreted as saying that the covalency between the copper and the ligand in the Jager complex is intermediate between the above two groupings of square-planar copper complexes.

Esr studies were also carried out on both VOA^1B^3 and $(VO)_2A^4(B^3)_2$. The esr spectrum of a $CHCl_3$ solution of VOA^1B^3 at room temperature is shown in Figure 8. The spectrum shows the expected eight vanadium hyperfine lines with $A_{av} = 92 \pm 2 \times 10^{-4}$ cm^{-1} and $g_{av} = 1.964$. A further characterization can be gained by doping the vanadyl complex. A 1% doped VOA^1B^3 (in diamagnetic NiA^1B^3) esr spectrum at liquid-nitrogen temperature is shown in Figure 9. Both the parallel and the perpendicular regions can now be seen with the eight vanadium hyperfine lines for each region; part of the parallel region overlaps the perpendicular region. The parallel region starts at a lower field than the perpendicular region and its last three components can be seen at a higher field than the perpendicular region. The esr spectrum of doped VOA^1B^3 was simulated with a computer program and the best fit parameters were found to be $g_{\parallel} = 1.947$, $g_{\perp} = 1.973$, $A_{\parallel} = 154.2 \pm 1 \times 10^{-4}$ cm^{-1}, and $A_{\perp} = 51.4 \pm 1 \times 10^{-4}$ cm^{-1}.

Difficulty was encountered in obtaining an esr spectrum of $(VO)_2A^4(B^3)_2$. The esr of the solid sample containing a small amount of DPPH gave a $g_{\perp}$ value of 1.959. An esr spectrum of a $CHCl_3$ solution of $(VO)_2A^4(B^3)_2$ at room temperature is shown in Figure 10. The g_{av} measured from this spectrum is 1.969. Eight vanadium hyperfine lines can be seen and A_{av} can be determined to be $97 \pm 3 \times 10^{-4}$ cm^{-1}. If an exchange interaction between the two vanadium atoms was present, 15 lines would be expected. In an attempt to obtain a spectrum exhibiting both the parallel and the perpendicular regions for $(VO)_2A^4(B^3)_2$, the compound was

(24) K. W. H. Stevens, *Proc. Roy. Soc., Ser. A*, 214, 237 (1952).
(25) D. Kivelson and R. Neiman, *J. Chem. Phys.*, 35, 149 (1961).

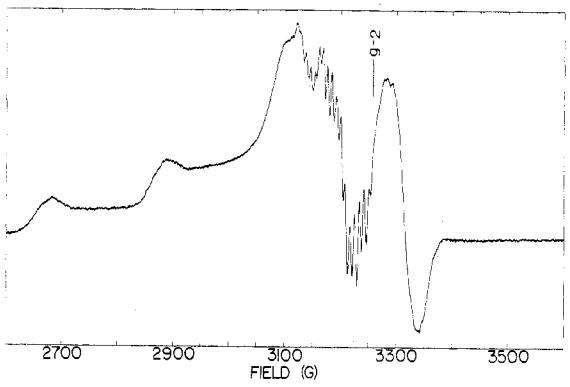

Figure 7. Esr spectrum of $Cu_2A^3(B^3)_2$ magnetically diluted in $A^3(B^3)_2H_4$ recorded at liquid-nitrogen temperature.

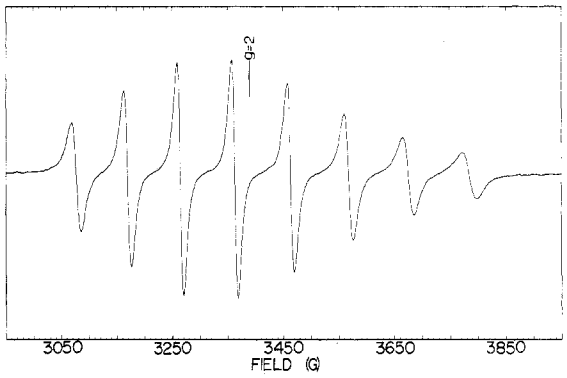

Figure 8. Esr spectrum of a VOA^1B^3 solution in $CHCl_3$ recorded at room temperature.

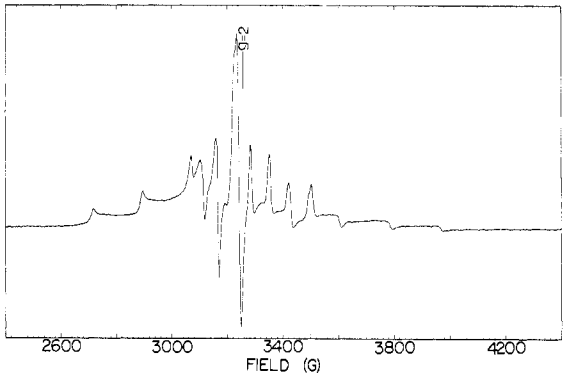

Figure 9. Esr spectrum of VOA^1B^3 magnetically diluted in NiA^1B^3 recorded at liquid-nitrogen temperature.

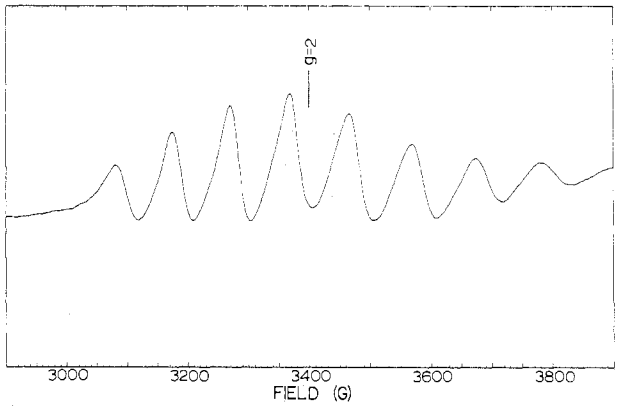

Figure 10. Esr spectrum of a $(VO)_2A^4(B^3)_2$ solution in $CHCl_3$ recorded at room temperature.

doped into both the ligand $A^4(B^3)_2H_4$ and $Ni_2A^4(B^3)_2$ at concentrations of 1 and 5%. In both cases spectra very similar to that of the doped VOA^1B^3 compound were obtained. This was puzzling in that even if there was no exchange interaction between the vanadium centers, there should still be zero-field splitting of a dipolar origin visible in the doped esr spectra of $(VO)_2A^4(B^3)_2$. It seems that the only explanation for the similarity of the doped $(VO)_2A^4(B^3)_2$ and doped $(VO)A^1B^3$ spectra lies in a chemical exchange that took place in the doping process. Exchange of VO^{2+} and Ni^{2+} ions occurred on one hand, while, in the attempt to dope into the ligand, the VO^{2+} in $(VO)_2A^4(B^3)_2$ equilibrated with the excess ligand and gave only $(VO)A^4(B^3)_2H_2$ and $A^4(B^3)_2H_4$ species. This problem was overcome by using frozen glass media for the vanadyl dimer. A frozen $CHCl_3$ solution of $(VO)_2A^4(B^3)_2$ gave poor resolution, partially as a result of low solubility. The compound was then dissolved in either DMSO or DMF and the frozen solution esr spectra were obtained; both solvents gave the same spectra. The liquid-nitrogen temperature frozen DMSO solution spectrum is shown in Figure 11. In the low-field parallel region of the spectrum the vanadium hyperfine lines can be seen to be split into two lines with a spacing of $65 \pm 2 \times 10^{-4}$ cm^{-1}. We tentatively assign this splitting to dipolar zero-field splitting. The vanadium $A_\parallel$ value can be determined to be 159×10^{-4} cm^{-1}, which with A_{av} from the solution spectrum gives $A_\perp = 66 \pm 2 \times 10^{-4}$ cm^{-1}. The 32.5×10^{-4} cm^{-1} zero-field splitting for $(VO)_2A^4(B^3)_2$ seems quite reasonable in that it gives a vanadium-vanadium distance of 8.66 Å, which is not dramatically different from that calculated for the copper dimer.

The esr parameters given in Table V are very similar to those reported by Kivelson and Lee[26] for various VO^{2+} complexes. These workers also developed theoretical expressions pertaining to VO^{2+} esr spectra and demonstrated that the unpaired electron was localized mainly on the vanadium ion. In fact, only the esr spectrum of vanadyl porphyrin showed extrahyperfine structure due to the ligand (nitrogen) atom and even in this case the splitting was small (~2.8 G).

Exchange Mechanism. The question at hand is why does $Cu_2A^4(B^3)_2$ possess an intramolecular exchange interaction, whereas $Cu_2A^3(B^3)_2$ and $(VO)_2A^4(B^3)_2$ do not. It is beneficial to first recall in brief what is meant by saying that a system possesses an exchange interaction. In terms of an effective spin Hamiltonian it means that for the isotropic case there is a term $J\hat{S}_1 \cdot \hat{S}_2$ representing the interaction between the two paramagnetic centers in the dimer. The corresponding real Hamiltonian term is a summation of exchange-type integrals resulting from the $\hat{e}^2/r_{ij}$ operator and antisymmetric wave functions. Electron repulsion of the exchange type is the essence of the $J\hat{S}_1 \cdot \hat{S}_2$ interaction. A calculation of the exchange interaction in a given paramagnetic metal dimer would involve an evaluation of the exchange terms for the ground state determinantal wave function and exchange terms from configuration interaction with various excited states. Normally this is not practical and one is reduced to a qualitative explanation of differences in exchange interaction. In a dimeric metal complex the superexchange mechanism can be discussed in terms of spin polarization between the unpaired electrons "localized" on the metal centers and the electrons "localized" on the bridge. The exchange integral J reflects the *net* interaction; that is, there are many pathways of spin polarization possible.

(26) D. Kivelson and S.-K. Lee, *J. Chem. Phys.*, 41, 1896 (1964).

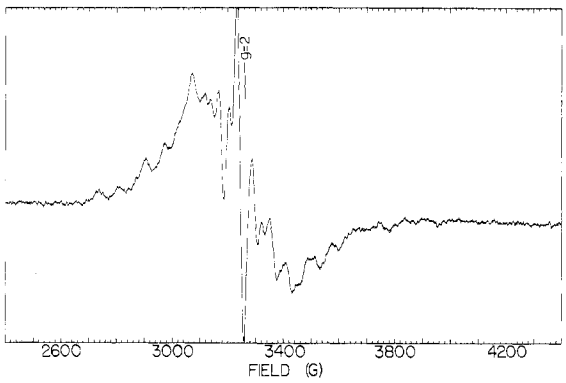

Figure 11. Esr spectrum of a frozen DMSO solution of $(VO)_2A^4(B^3)_2$ recorded at liquid-nitrogen temperature.

If we label the molecular plane of a square-planar copper complex as the xy plane with the x and y axes directed at the ligands, then it is evident[25] that the unpaired electron is present in a b_{1g}* (D_{4h} symmetry assumed) molecular orbital ($d_{x^2-y^2}$ atomic orbital). The unpaired copper electron is in an orbital directed at the ligands and as a consequence the esr spectra for doped samples of CuA^1B^3 and $Cu_2A^4(B^3)_2$ exhibit nitrogen as well as hydrogen hyperfine. Even further, the $A_\parallel$(Cu) is relatively large for these two copper complexes indicating a fair amount of metal-ligand covalency. The antiferromagnetic exchange interaction in $Cu_2A^4(B^3)_2$ can thus be viewed as resulting from a spin polarization between the unpaired "copper" electron and the various nitrogen electrons, a polarization that is propagated through the benzene moiety to the other copper atom. The N_2O_2 environment in $Cu_2A^4(B^3)_2$ approximates C_{2v} symmetry, in which case the copper $d_{x^2-y^2}$ orbital is of a_1 symmetry. A CNDO/2 molecular orbital calculation for

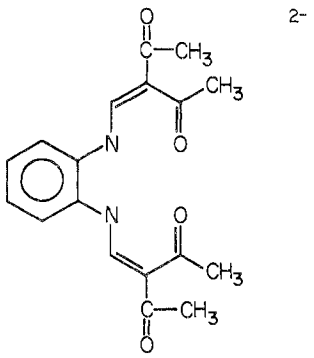

shows that there are many low-energy a_1 symmetry ligand molecular orbitals available as potential exchange pathways in $Cu_2A^4(B^3)_2$.

There is no exchange interaction evident in $Cu_2A^3(B^3)_2$ which has a biphenyl bridging moiety. In this case it is clear from the esr work that the covalency between the copper atoms and the ligands is comparable to that in $Cu_2A^4(B^3)_2$. The explanation for the absence of an interaction in $Cu_2A^3(B^3)_2$ must lie in the ability of the bridging moiety to propagate a spin polarization. It seems that spin polarization would be attenuated with distance or perhaps there is little spin polarization between the two phenyl groups in the biphenyl bridge. The carbon-carbon bond between the two rings in biphenyl is known[27] to be a single bond (distance = 1.5 Å).

The absence of an exchange interaction in $(VO)_2A^4(B^3)_2$

(27) A. Hargreaves and S. H. Rizvi, *Acta Crystallogr.*, 15, 365 (1962).

is readily explained. In this case the unpaired vanadyl electron is in an a_2 symmetry molecular orbital (d_{xy} vanadium orbital). This molecular orbital is in the molecular plane but is not directed at the ligand atoms. The esr spectra for $(VO)_2A^4(B^3)_2$ showed that the a_2 orbital in which the unpaired electron resides is dominantly vanadium in composition. There is little spin polarization into the tetraaminobenzene moiety and thus no apparent exchange interaction between the vanadium centers.

Experimental Section

Compound Preparation. The analytical data for all compounds appear in Table I. Complexes of the mononucleating ligands A^1B^3, A^1B^1, A^2B^1, and A^2B^3 were prepared according to the method reported by Jager.[15]

Preparation of $A^4(B^3)_2H_4$. 1,2,4,5-Tetraaminobenzene tetrahydrochloride was purchased from Burdick and Jackson. The free amine was obtained according to the method of Vogel and Marvel.[28] The 1,2,4,5-tetraaminobenzene will decompose if exposed to air for a relatively short period of time; thus, it was used immediately after preparation. The preparation of $A^4(B^3)_2H_4$ was then carried out in the same manner as reported for the Jager monomers. The compound was obtained as a bright yellow powder (mp 252°).

Preparation of $A^3(B^3)_2H_4$. 3,3',4,4'-Tetraaminobiphenyl was purchased from Burdick and Jackson as the free base. It was recrystallized from hot methanol prior to its use. The preparation of $A^3(B^3)_2H_4$ was also carried out in the same manner as reported for the Jager monomers. The compound was obtained as a bright yellow powder (mp 246°).

Preparation of Cu(II) and Ni(II) Complexes. Dissolution of $A^4(B^3)_2H_4$ and $A^3(B^3)_2H_4$ in hot methanol was effected by adding a fourfold amount of potassium *tert*-butoxide to a hot methanol slurry of the ligand. To this solution a hot methanol solution of the hydrated metal acetate was added. The complexes precipitated out of solution immediately. The solution was filtered and the precipitate was washed several times with methanol and ether and then dried *in vacuo* over P_2O_5. The copper complex was obtained as a fine dark brown powder and the nickel complex as a fine dark orange powder. The melting points of these compounds are above 300°.

Preparation of $(VO)_2A^4(B^3)_2$. To a hot methanol solution (obtained as above) of the ligand, a hot methanol–water solution of $VOSO_4 \cdot 2H_2O$ was added. The compound $(VO)_2A^4(B^3)_2$ is very soluble in methanol, and thus the precipitated K_2SO_4 was filtered out and the solution allowed to evaporate to dryness. The vanadyl dimer was then recrystallized from methanol, washed with ether, and dried *in vacuo* over P_2O_5. The compound was obtained as a fine reddish brown powder with a melting point higher than 300°.

Physical Measurements. The infrared spectra were obtained on a Perkin-Elmer Model 457 spectrophotometer. Samples were run as KBr pellets from 4000 to 250 cm^{-1}. Potassium bromide of Spectrograde quality was purchased from Harshaw Chemical Co. and was dried in an oven at 110° before use.

Low-resolution mass spectra were recorded with a Varian CH-5 mass spectrometer with the following operating conditions: acceleration voltage, 3 kV; electron energy, 70 V; emission current, 100 μA; resolution, 800; electron multiplier, 1.75 kV [2.0 kV for $Cu_2A^4(B^3)_2$]; analyzer pressure, 10^{-7} Torr. The solid sample rod was heated to temperatures between 390 and 500° depending on sample volatility. A computer program for the prediction of isotope patterns for mass spectra peaks was provided by Professor Edward Carberry (Southwest Minnesota State College).

Variable-temperature (4.2–290°K) magnetic susceptibility measurements were carried out with a Princeton Applied Research Model 150A vibrating sample magnetometer. The superconducting magnet was operated at 54.3 kG. A calibrated gallium arsenide diode was used as a temperature controlling and sensing device. For all measurements $CuSO_4 \cdot 5H_2O$ was used as a standard. Corrections were made at all temperatures for the diamagnetism of the sample container and background. Pascal constants were used to correct for the diamagnetism of the compounds. A least-squares fitting of the magnetic susceptibility curve for $Cu_2A^4(B^3)_2$ was carried out using STEPT, a computer function minimization program written by J. P. Chandler (Indiana University).

Esr spectra were obtained using a Varian E-9 spectrometer at X-band frequencies. A Varian Model 4540 variable-temperature controller was used to determine the temperature. All spectra were taken at liquid-nitrogen temperature with the exception of the solution spectra for CuA^1B^3, VOA^1B^3, and $(VO)_2A^4(B^3)_2$ which were taken at room temperature. To the pure solid samples a small amount of DPPH was added to accurately determine the $g_\perp$ values. The "doped" samples were made by dissolving a small amount of the paramagnetic complex in DMF, adding this solution to a DMF solution of the corresponding diamagnetic nickel complex at room temperature, and then evaporating in a Rinco rotating vacuum-type evaporator until enough doped compound appeared in solution. The solution was then filtered and the precipitate washed several times with ether and dried *in vacuo* over P_2O_5. For the copper complexes a 1:1000 dilution and a 1:100 dilution were made, for the vanadyl monomer the ratio was 1:100, and for the vanadyl dimer both 1:100 and 5:100 ratios were used. For the solution spectra of CuA^1B^3, VOA^1B^3, and $(VO)_2A^4(B^3)_2$ at room temperature, reagent grade chloroform was used, and for the frozen solution spectra of $(VO)_2A^4(B^3)_2$ reagent grade DMSO and DMF were used. All samples were loaded into quartz tubes and sealed under vacuum (∼10 μ); solutions were degassed prior to sealing the tubes under vacuum.

Acknowledgment. Financial support was derived from NIH Grant HL 13652. We are grateful for helpful discussions with Professor R. L. Belford. The mass spectral data processing equipment employed in the present study was provided by NIH Grants CA 11388 and GM 16864 from the National Cancer Institute and the National Institute of General Medical Sciences, respectively. The Varian Model E-9 esr spectrometer was purchased in part with a NSF departmental grant.

Registry No. $A^1B^3H_2$, 40895-08-7; CuA^1B^3, 40895-09-8; CuA^1B^1, 40895-10-1; CuA^2B^3, 40895-11-2; CuA^2B^1, 40959-47-5; NiA^1B^3, 40895-12-3; VOA^1B^3, 40895-13-4; $A^4(B^3)_2H_4$, 40895-14-5; $Cu_2A^4(B^3)_2$, 40895-15-6; $Ni_2A^4(B^3)_2$, 40895-16-7; $(VO)_2A^4(B^3)_2$, 40895-17-8; $A^3(B^3)_2H_4$, 40895-18-9; $Cu_2A^3(B^3)_2$, 40895-19-0; $CuNiA^4(B^3)_2$, 41086-69-5.

(28) H. Vogel and C. S. Marvel, *J. Polym. Sci.*, **50**, 511 (1961).